Inorganic Chemistry

Article

pubs.acs.org/IC

Influence of the Synthesis Parameters onto Nucleation and Crystallization of Five New Tin−Sulfur Containing Compounds

Jessica Hilbert, Christian Näther, and Wolfgang Bensch*

Institute of Inorganic Chemistry, Christian-Albrechts-University of Kiel, Max-Eyth-Str. 2, Kiel 24118, Germany

Supporting Information

ABSTRACT: The distinct control of the synthesis parameters achieved crystallization of five new inorganic−organic hybrid tin sulfides with 1,10-phenanthroline (phen) as the organic component: $\{[Mn(phen)_2]_2(\mu_2\text{-}Sn_2S_6)\}$ (**1**, **3**), $\{[Mn(phen)_2]_2(\mu_2\text{-}Sn_2S_6)\}\cdot phen$ (**2**), $\{[Mn(phen)_2]_2(\mu_2\text{-}Sn_2S_6)\}\cdot phen\cdot H_2O$ (**4**), and $\{[Mn(phen)_2]_2[\mu\text{-}\eta^2\text{-}\eta^2\text{-}SnS_4]_2[Mn(phen)]_2\}\cdot H_2O$ (**5**). Compounds **1**, **3**, and **4** occur successively under static conditions by increasing the reaction time up to 8 weeks. Stirring the reaction mixtures and keeping the educt ratio constant allow preparation of distinct phase pure samples within very short reaction times. At higher autogenous pressure, crystallization and conversion of several compounds are suppressed, and only **1** crystallized. Compound **2** could only be obtained in glass tubes at low pH value of the reaction mixture or at low amine concentration. Adjusting the pH value of the solution, the concentration, and the volume of the solvent, compounds **1**−**4** crystallize sequentially and were successively converted into each other. Results of thermal stability experiments and solubility studies suggest that compounds **1** and **3** are polymorphs following the density rule. Compounds **2** and **4** may be viewed as pseudopolymorphs of **1** and **3**.

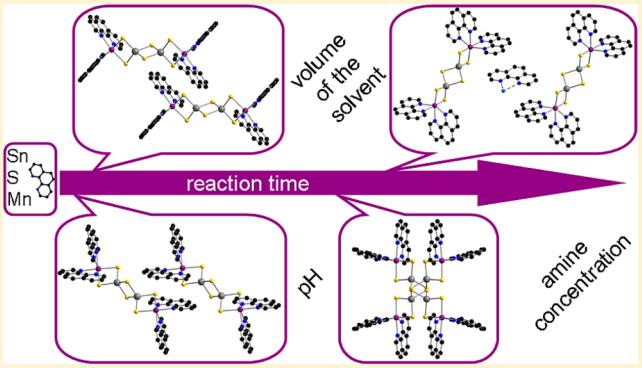

INTRODUCTION

During the last decades, a huge variety of thiometalate compounds were prepared by the solvothermal route, and the intriguing chemistry of these compounds has been discussed in various review articles.[1−5] Thiostannates are an attractive group of compounds among the main group thiometalates, and they are promising candidates for catalysis, sensors, absorbers, and ion exchangers.[6−9] Alteration of physicochemical properties of thiostannates can be achieved by integration of transition metal cations (TMCs) into the networks.[10] In most cases, the syntheses are performed under solvothermal conditions,[11−14] and due to the multidimensional parameter space, controlling product formation is a challenging task. Many parameters, for example, kind of educts, reaction time and temperature, concentration of the solvent, type of solvent, pH value, redox potential, autogenous pressure, and viscosity of the solvent, influence the product formation. In addition, changing only one parameter alters others in a not well-controlled way. Another drawback of solvothermal syntheses done under static conditions (no stirring of the mixture) is the development of strong concentration gradients that may lead to the nucleation and growth of different phases. On the other hand, crystals are obtained under these conditions that are suitable for single-crystal X-ray work. A critical review of the synthesis conditions reported in a large number of papers reveals that, in the overwhelming cases, reaction times were chosen between 3 and about 7 days. Keeping in mind that the reaction conditions of solvothermal syntheses are mild enough to obtain metastable or kinetically stabilized products, one can expect that the least stable compound crystallizes first followed by the more stable compound(s) (Ostwald's rule). The energetic difference between the different compounds is often small and can be overcome by extending the reaction time. This approach was demonstrated by us to be successful in the thioantimonate chemistry.[15] Because solvothermal syntheses are often performed in steel autoclaves, an optical control of reaction progress as a function of time is not possible, but also, reactions undertaken in glass tubes do not allow online identifying crystallization of different compounds as a function of the reaction time. However, the occurrence of crystalline intermediates/metastable compounds, their interconversion, and their crystal growth can be studied using suitable *in situ* techniques like X-ray diffraction performed with synchrotron radiation sources.[16,17a−e] Disadvantages of such experiments are the time restriction and the large experimental effort. Until now, several hybrid thiostannates have been synthesized with predominantly TMCs coordinated by aliphatic amine molecules. Using π-conjugated ligands for TMC complexation, specific photochemical and electrochemical properties can be expected.[18] A promising ligand is 1,10-phenanthroline (phen) that was used for the generation of new thiostannates.[19]

Received: February 17, 2014
Published: May 20, 2014

   dx.doi.org/10.1021/ic500369m | *Inorg. Chem.* 2014, 53, 5619−5630

Table 1. Selected Details of the Data Collection and Structure Refinement Results

	1	3	2	4	5
crystal system	monoclinic	monoclinic	triclinic	triclinic	triclinic
space group	$P2_1/n$	$C2/c$	$P\bar{1}$	$P\bar{1}$	$P\bar{1}$
M (g/mol)	1260.44	1260.44	1440.64	1458.66	1812.86
a (Å)	10.8230(4)	25.6736(7)	10.0642(9)	11.3203(7)	10.8703(5)
b (Å)	9.8940(2)	11.1006(4)	10.6249(9)	12.1436(7)	12.5183(6)
c (Å)	24.8107(10)	18.0647(5)	13.6927(12)	12.7586(7)	14.9644(6)
α (deg)	90.0	90.0	71.700(7)	113.200(4)	103.381(3)
β (deg)	91.356(3)	98.164(2)	81.458(7)	90.908(5)	108.390(3)
γ (deg)	90.0	90.0	84.346(7)	111.974(4)	101.636(4)
V (Å^3)	2656.05(15)	5096.1(3)	1372.6(2)	1479.92(15)	1794.71(14)
Z	4	4	1	1	1
$D_{calculated}$ (g/cm^3)	1.576	1.643	1.743	1.637	1.677
μ (mm^{-1})	1.670	1.741	1.629	1.513	1.654
scan range (deg)	$1.64 \le \theta \le 24.62$	$2.00 \le \theta \le 27.00$	$1.58 \le \theta \le 22.78$	$1.77 \le \theta \le 27.00$	$1.51 \le \theta \le 27.00$
reflections collected	28 044	22 159	11 651	13 856	18 641
independent reflections	4454	5496	11 661	6406	7768
observed reflections	3840	4972	8029	4952	6507
goodness-of-fit on F^2	1.373	1.095	1.027	0.938	1.079
final R indices (I > 2σ(I))	$R1$ = 0.0428	$R1$ = 0.0264	$R1$ = 0.0634	$R1$ = 0.0284	$R1$ = 0.0412
	$wR2$ = 0.1045	$wR2$ = 0.0574	$wR2$ = 0.1115	$wR2$ = 0.696	$wR2$ = 0.1039
R indices (all data)	$R1$ = 0.0517	$R1$ = 0.0322	$R1$ = 0.1046	$R1$ = 0.0432	$R1$ = 0.0534
	$wR2$ = 0.1078	$wR2$ = 0.0593	$wR2$ = 0.1242	$wR2$ = 0.0731	$wR2$ = 0.1084
res. elec. dens. (e/Å^3)	0.566 and −0.681	0.301 and −0.326	0.971 and −0.876	0.653 and −0.660	0.972 and −0.720

In the present contribution, we report results of the investigation of the Mn/Sn/S/phen system and synthesized four new inorganic−organic hybrid compounds under static conditions with the $[Sn_2S_6]^{4-}$ anion connecting Mn^{2+} centered complex cations into the $\{[Mn(phen)_2]_2(Sn_2S_6)\}$ unit as the main structural motif. Three of these compounds ($\{[Mn(phen)_2]_2(Sn_2S_6)\}$ (**1** and **3**) and $\{[Mn(phen)_2]_2(Sn_2S_6)\}\cdot phen\cdot H_2O$ (**4**)) were discovered by increasing the reaction time from 5 days to 8 weeks. The occurrence of **1** and **3** as a function of reaction time is a nice example for Ostwald's rule.[20,21] Compound **5**, $\{[Mn(phen)_2]_2(SnS_4)_2[Mn(phen)]_2\}\cdot H_2O$, features a tetradentate acting $[SnS_4]^{4-}$ ion exhibiting a hitherto not observed binding mode and could only be isolated applying static reaction conditions. We then performed solvothermal reactions under dynamic conditions (stirring of the reaction slurries) applying always identical educt ratios of the Mn, Sn, and S sources and varying the reaction conditions. Under these conditions $\{[Mn(phen)_2]_2(Sn_2S_6)\}\cdot phen$ (**2**) crystallized at a lower pH value using a glass tube as the reaction container. Interestingly, compounds **1**−**4** were obtained within a few hours as phase pure materials adjusting the amine concentration, reaction time, temperature, autogenous pressure, and/or pH value, while compound **5** did not crystallize under these conditions.

EXPERIMENTAL SECTION

Synthesis. *General.* All chemicals were purchased and used without further purifications. All compounds were prepared under solvothermal conditions in glass tubes (inner volume 11 mL) or Teflon-lined steel autoclaves (inner volume 30 mL) using $MnCl_2\cdot 4H_2O$, Sn, S, and phen. Further details of the syntheses are summarized in Tables S1 and S2 (Supporting Information). The crystalline products were filtered off after the reactions, washed with water and ethanol, and dried in vacuum. The reaction products were separated manually, and the homogeneity was checked by X-ray powder diffraction (XRPD) and elemental analysis. Experimental and calculated XRPD patterns are shown in Figure S1 (Supporting Information). For the dynamic syntheses, the products were not separated, but the composition of product mixture was evaluated by XRPD.

Reactions in Teflon-Lined Steel Autoclaves under Static Conditions. A 1.57 (0.79) mmol of $MnCl_2\cdot 4H_2O$, 0.79 (0.79) mmol of Sn, 3.14 (2.37) mmol of S, and 0.79 (1.58) mmol of phen were reacted with 6.28 mL of solvent under static conditions at 120 and 150 °C. Solvent compositions in detail: methylamine (ma) (30%): 3.96 mL of ma (40%, aqueous solution, abcr) and 1.32 mL of deionized water; butylamine (ba) (100%): 6.28 mL of ba (≥98%, Fluka); and ba (50%): 2.64 mL of ba (≥98%, Fluka) and 2.64 mL of deionized water.

Reactions in Glass Tubes under Static Conditions. A 0.5 (0.25) mmol of $MnCl_2\cdot 4H_2O$, 0.25 (0.25) mmol of Sn, 1.0 (0.75) mmol of S, and 0.25 (0.5) mmol of phen were reacted with 2 mL of solvent under static conditions at 120 °C. The synthesis could not be carried out at 150 °C because the screw caps were not stable at this temperature. Solvent compositions in detail: ma (30%): 1.5 mL of ma (40%, aqueous solution, abcr) and 0.5 mL of deionized water; ethylamine (ea) (50%): 1.42 mL of ea (70%, aqueous solution Fluka) and 0.58 mL of deionized water; *n*-propylamine (npa) (100%): 2 mL of npa (99% Merck−Suchardt); npa (50%): 1 mL of npa (99% Merck−Suchardt) and 1 mL of deionized water; ba (100%); and ba (50%): 1 mL of ba and 1 mL of deionized water. A short overview of the reaction conditions of the syntheses performed under static conditions can be found in Table S1 (Supporting Information).

Dynamic Syntheses in Glass Tubes. A 0.2 mmol of $MnCl_2\cdot 4H_2O$, 0.2 mmol of Sn, 0.6 mmol of S, and 0.4 mmol of phen with methylamine solution (ma; 40%, aqueous solution, abcr) were reacted in a 7 mL glass tube under stirring conditions (magnetic stirrer) at T = 120, 140, and 150 °C up to 20 h. An overview of the used solvent mixtures and their resulting pH values are given in Table S2 (Supporting Information). To exclude any influence of the stirring speed on nucleation and crystal growth, in all experiments, the same magnetic stirrer was used with a fixed stirring speed.

Single-Crystal Structure Determination. The intensity data for the compounds were collected using a STOE IPDS-1 (Imaging Plate Diffraction System) with Mo Kα radiation (λ = 0.07107 Å) at room temperature. The structures were solved with direct methods using the program SHELXS-97[22], and the refinements were done against F^2 with SHELXL-97.[23]

dx.doi.org/10.1021/ic500369m | Inorg. Chem. 2014, 53, 5619−5630

All non-hydrogen atoms except those of the disordered uncoordinated phen ligand in compound **2** were refined anisotropic. The C−H hydrogen atoms were positioned with idealized geometry and refined isotropic using a riding model. For all compounds, a numerical absorption correction was performed. All crystals investigated for compound **2** where nonmerohedral twinned. This twinning unfortunately leads to reflections along the *c* axis, which cannot be resolved. Therefore, data were measured to only $2\theta = 45°$, and the structure was refined using the HKLF-5 option. Unfortunately, by using this procedure, the equivalent reflections cannot be merged, and therefore, the number of independent reflections is artificially too large. If the overlapping reflections are omitted, the completeness is less than 60% which is inacceptable. The structure can easily be solved in space groups *P*1 and $P\bar{1}$. In space group *P*1, the displacement factors of several atoms are nonpositive defined, and the Flack *x* parameter is always about 0.5. Large correlations of the parameters are observed indicating the presence of a center of symmetry. Even if the uncoordinated phen ligand seems to be ordered in *P*1, Platon immediately suggest space group $P\bar{1}$ in which this ligand is disordered around a center of inversion. Therefore, space group $P\bar{1}$ was selected for the final refinements. In compound **4**, the water H atoms were not located but considered in the formula. One phen ligand is disordered around a center of inversion, in which also one water molecule is involved. Both of them were refined with half occupancy. The disorder remains if the structure refinement is performed in space group $P\bar{1}$, where all atoms are located in general positions. After structure refinement for compound **5**, there was one remaining small electron density maximum to which a half-occupied water molecule was assigned. Additional residual electron density peaks were located, which can be assigned to the water H atoms. The O−H H distances were set to ideal values and finally the H atoms were refined using a riding model.

Selected refinement results are summarized in Table 1. Structural data have been deposited in the Cambridge Crystallographic Data Centre as publication nos. CCDC 999247 (**1**), CCDC 999248 (**2**), CCDC 999249 (**3**), CCDC 999250 (**4**), and CCDC 999251 (**5**). Copies of the data can be obtained, free of charge, on application to CCDC, 12 Union Road, Cambridge CB2 1 EZ, UK (deposit@ccdc.ca.ac.uk).

X-ray Powder Diffractometry. The XRPD patterns were recorded on a STOE Stadi-P powder diffractometer (Cu $K\alpha_1$ radiation, λ = 1.540598 Å, Ge monochromator) in transmission geometry.

Investigation of the samples during heating was done by *in situ* X-ray diffractometry (PANalytical X'Pert Pro diffractometry, Cu $K\alpha$ radiation, Göbel mirror at the incident beam, PIXel detector, step size 0.03). The *in situ* measurements were carried out in a high-temperature chamber (HTC, Anton Paar HTK 1200N) under helium atmosphere with a heating rate of 4 °C/min and held at constant temperature during the measurement.

Energy Dispersive X-ray Experiments. Scanning electron microscopy investigations and energy dispersive X-ray (EDX) analyses were done with a Philips environmental scanning electron microscope ESEM XL30 equipped with an EDAX detector.

Spectroscopic Properties. *UV/visible Spectroscopy.* UV/visible (UV/vis) spectroscopic investigations were carried out at room temperature using an UV/vis/NIR two-channel spectrometer Cary 5 from Varian Techtron Pty., Darmstadt. The optical properties of compounds **1**−**5** were investigated by analyzing the UV/vis reflectance spectra of the powdered samples (with $BaSO_4$ powder used as reference material). The absorption data were calculated applying the Kubelka−Munk relation for diffuse reflectance data (see Figure S2, Supporting Information).

Infrared Spectroscopy. MIR spectra (400−3500 cm^{-1}) were recorded with an ATI Mattson Genesis spectrometer (see Figure S3 and Table S3, Supporting Information).

Raman Spectroscopy. Raman spectra were recorded with a Bruker IFS 66 Fourier transform spectrometer (wavelength: 541.5 nm) in the range from 100 to 3500 cm^{-1} (see Table S4 and Figure S4, Supporting Information).

Atomic Absorption Spectroscopy. Atomic absorption spectroscopy (AAS) was performed with a PerkinElmer Analyst 3000 system.

RESULTS AND DISCUSSION

Synthetic Aspects. The five new compounds were obtained during a systematic investigation of the influence of the synthesis parameters onto product formation applying static conditions. The reproducibility of the results was verified by performing each synthesis several times. Only compounds **1**, **3**, **4**, and **5** could be obtained in Teflon-lined autoclaves under static conditions. Compound **1** could be identified up to 21 days of reaction time, compounds **3** and **4** crystallized between 21 and 30 days, and for even longer reaction times, only **4** could be observed. Remarkably, besides **1**, **3**, and **4**, another compound (**2**) crystallized at T = 120 °C using glass tubes as a reaction container and adjusting the pH value to 11. There are two remarkable differences between the two types of containers: the volume and the roughness of the surface. While the surface of the glass tubes is relatively smooth, that of the Teflon-liner is rough and porous. These two factors may be important for nucleation and crystallization of a distinct compound. One can only speculate whether heterogeneous nucleation is favored using Teflon as the container and homogeneous nucleation occurs in the glass tubes. In this context, it is noted that, in all investigations, always new Teflon-liner were used to avoid any cross-contamination. Indeed the Teflon-liners are used several times but only for the same chemical system. Another interesting result obtained during the studies is that several compounds transform into others as a function of the reaction time.

In the following, we first present the crystal structures of the new compounds grouped according to the different structural building units. Compound **5** does not contain the $[Sn_2S_6]^{4-}$ anion but was obtained during our systematic study, and therefore, we include the structure in our discussion. In the next section, we then discuss the results of the syntheses performed under dynamic conditions.

Crystal Structures of Compounds 1−4. In the structures of **1**−**4**, the $[Mn(phen)_2]^{2+}$ complex is a central structural motif. The Mn^{2+} ion has two bonds to S atoms of the $[Sn_2S_6]^{4-}$ anion and four bonds to N atoms of the phen ligands, thus forming distorted $[MnN_4S_2]^{2+}$ octahedra. The geometric parameters of the complexes such as Mn−N and Mn−S bond lengths as well as the angles around Mn^{2+} (Table S5, Supporting Information) are very similar in **1**−**4**, and match well with literature data.[10,19,24−26] The $[Sn_2S_6]^{4-}$ bitetrahedron is very common in thiostannates[10,25−36] and is formed by two edge-sharing SnS_4 tetrahedra. The geometric parameters of the $[Sn_2S_6]^{4-}$ anions in **1**−**4** display the typical bonding pattern with longer bridging Sn−S bonds and shorter bonds to the S atoms that are also bonded to Mn^{2+} (see Table S5, Supporting Information). Interestingly, the bond formation to Mn^{2+} does not significantly affect the Sn−S bonding pattern compared to the free $[Sn_2S_6]^{4-}$ anion as exemplified by comparison of the geometric parameters for compounds **1** and **3** with data of $Na_4Sn_2S_6{\cdot}14\ H_2O$ (see Table S6, Supporting Information).

In all compounds, all terminal S atoms of the $[Sn_2S_6]^{4-}$ anion have bonds to the Mn^{2+} centered complex. We note that, in most cases, this moiety is found as a discrete anion[37,38] or is acting as a bidentate ligand using the *trans* terminal S atoms.[10,37,38] The tetradentate bonding mode observed in **1**−**4** for the $[Sn_2S_6]^{4-}$ anion was never observed before and has been found so far only in the related class of selenidostannates

dx.doi.org/10.1021/ic500369m | Inorg. Chem. 2014, 53, 5619−5630

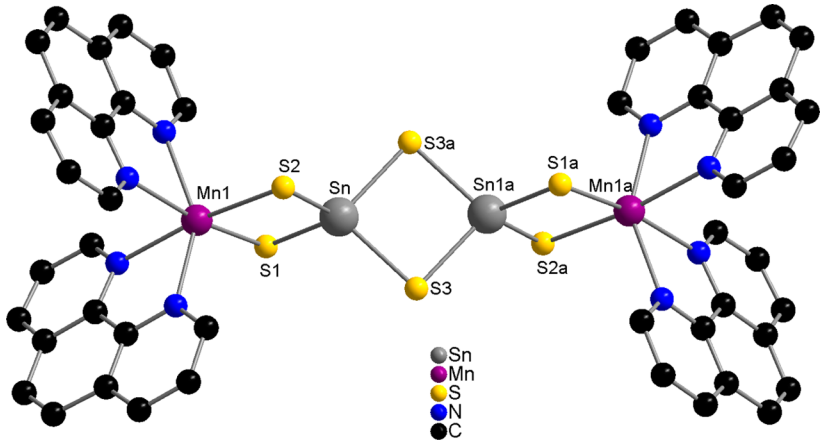

Figure 1. Structure of the $\{[Mn(phen)_2]_2(\mu_2\text{-}Sn_2S_6)\}$ moiety observed in compounds **1**–**4**. The hydrogen atoms are omitted for clarity.

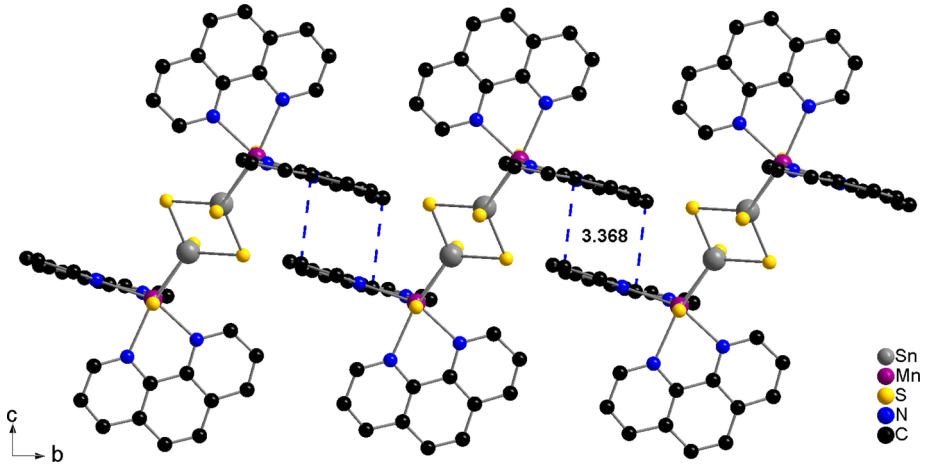

Figure 2. Parallel arrangement of the molecules in **1** along *b*, assembled by off-center parallel stacking (blue dashed lines) along *c*. Hydrogen atoms are omitted for clarity.

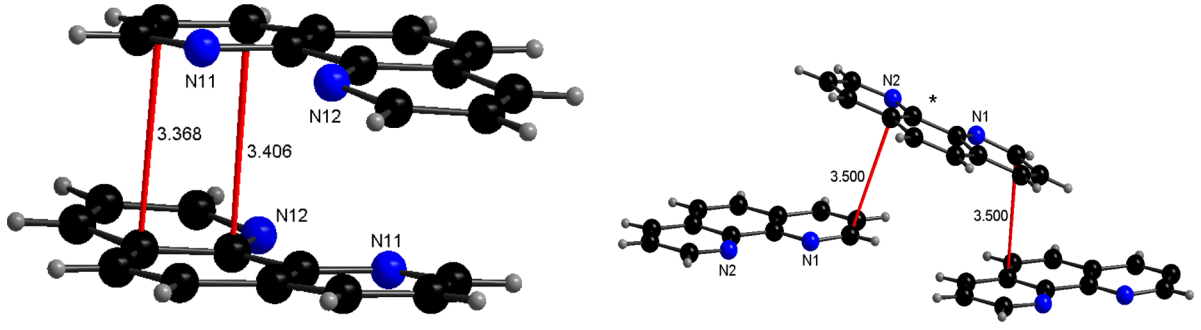

Figure 3. Two different arrangements of the phen molecules in the structure of **1**. The red lines with the numbers show the shortest intermolecular distances in Å.

where only few examples were reported.[14,39] Hence, in the structures of **1**–**4**, $\{[Mn(phen)_2]_2(\mu_2\text{-}Sn_2S_6)\}$ moieties are observed (Figure 1), and the different structures result from different packing of the constituents due to different stacking arrangements of the phen ligands. The dihedral angles between the phenantroline ligands are listed in Table S7 (Supporting Information). These values scatter around 90° by about ±10°.

Compound **1** (monoclinic, space group $P2_1/n$, $Z = 2$) is isostructural to $\{[Mn(phen)_2]_2(\mu_2\text{-}Sn_2Se_6)\}$[18] whereas compound **3** (monoclinic, space group $C2/c$, $Z = 4$) is isostructural to $\{[Fe(phen)_2]_2(\mu_2\text{-}Sn_2Se_6)\}$.[14]

In compound **1**, each $\{[Mn(phen)_2]_2(\mu_2\text{-}Sn_2S_6)\}$ unit interacts with adjacent molecules through off-center parallel stacking[40] between the phen ligands (3.369 Å) along the *c* axis (Figure 2). The molecules proceed along [100] and [010] (Figure 2 and Figure S5, Supporting Information) leading to formation of a two-dimensional (2D) layerlike arrangement within the *ab* plane. A three-dimensional (3D) network is generated by an off-center parallel arrangement along [001] (Figure S5, Supporting Information).

The energy involved in the stacking of the phen ligands was exemplarily calculated for compound **1**.[41−44] The two different

dx.doi.org/10.1021/ic500369m | Inorg. Chem. 2014, 53, 5619−5630

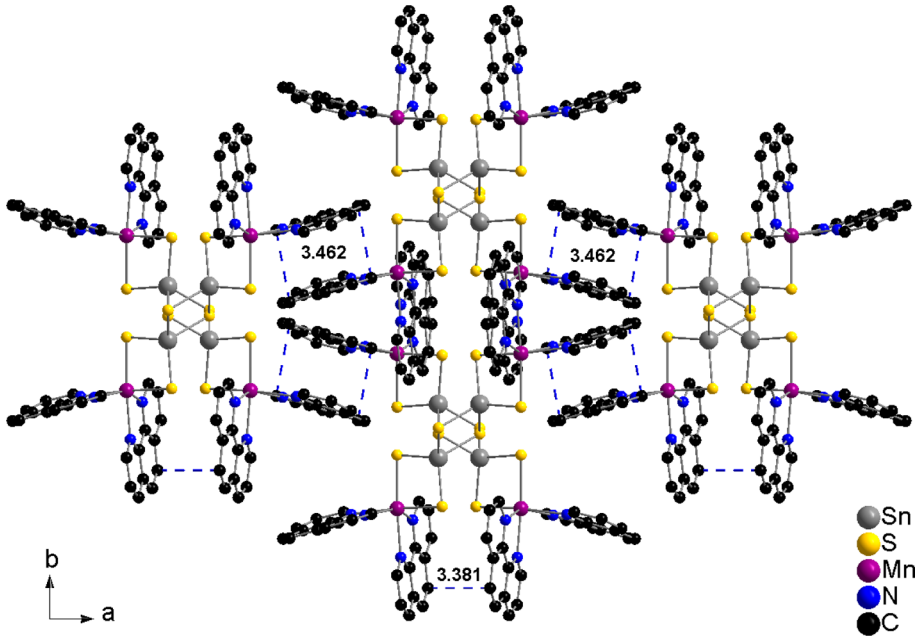

Figure 4. Antiparallel stacking of the layers along *c*; off-center parallel stacking (blue dashed lines) in **3** along the *a* and *b* axes. Hydrogen atoms are omitted for clarity.

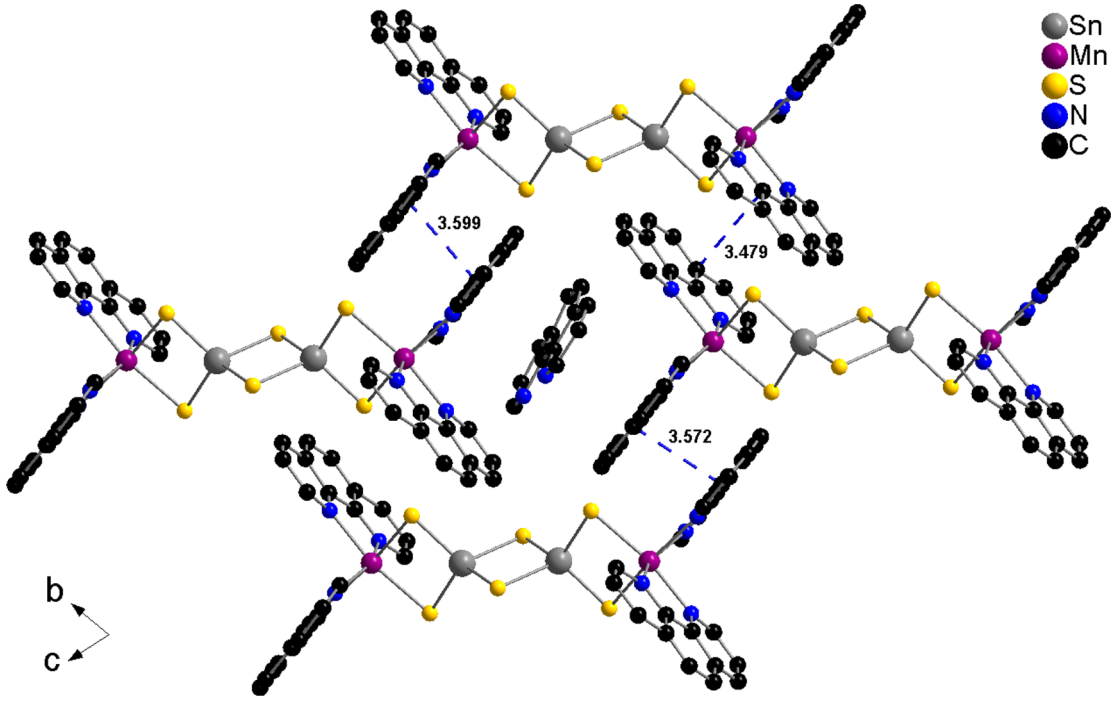

Figure 5. Arrangement of the molecules in **2** with off-center parallel orientation of the phen ligands (blue dashed lines) along *b* and *c*. Hydrogen atoms are omitted for clarity. Only one position of the disordered free phen molecule is displayed.

arrangements of the phen molecules were cut-out of the structure of **1** for the calculations (see Figure S5, Supporting Information). The energy obtained for the arrangement on the left in Figure 3 is 10.4 kcal/mol while the interaction energy of the phen ligand marked with an asterisk (Figure 3, right) with the two molecules below is about 13.4 kcal/mol. These values are in the typical range reported in the literature (e.g., see ref 42b). We note that the separations of the phen molecules in compounds **2**–**5** are in the same range observed for **1**, and therefore, it can be assumed that the interaction energies are also in the range calculated for this compound.

In compound **3**, each $\{[Mn(phen)_2]_2(\mu_2\text{-}Sn_2S_6)\}$ unit interacts also with adjacent molecules by two different off-center parallel stacking along [100] (3.381 Å) and along [010] (3.462 Å) leading to the formation of a layerlike arrangement within the (001) plane (Figure 4). The layers are antiparallel oriented along [001] and are joined by off-center parallel stacking along [100] (Figure 4).

dx.doi.org/10.1021/ic500369m | *Inorg. Chem.* 2014, 53, 5619–5630

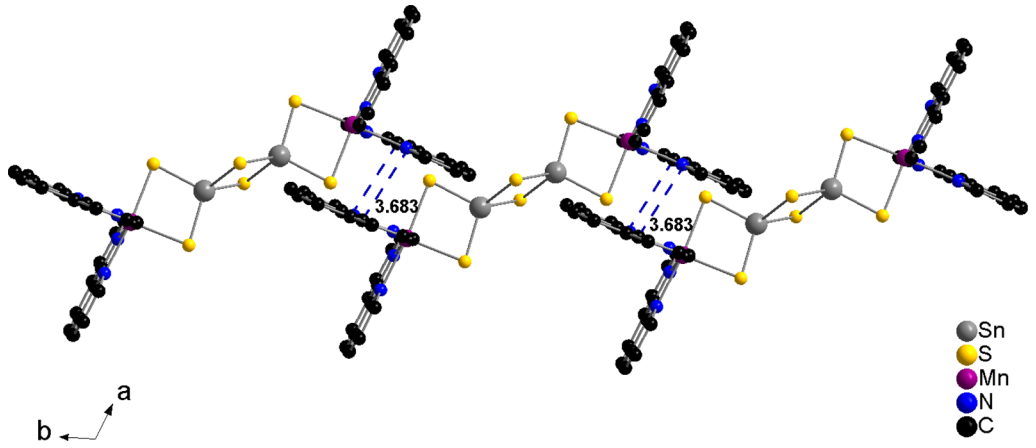

Figure 6. Chainlike arrangement of the $\{[Mn(phen)_2]_2(\mu_2\text{-}Sn_2S_6)\}$ units along the *b* axis. Hydrogen atoms are omitted for clarity.

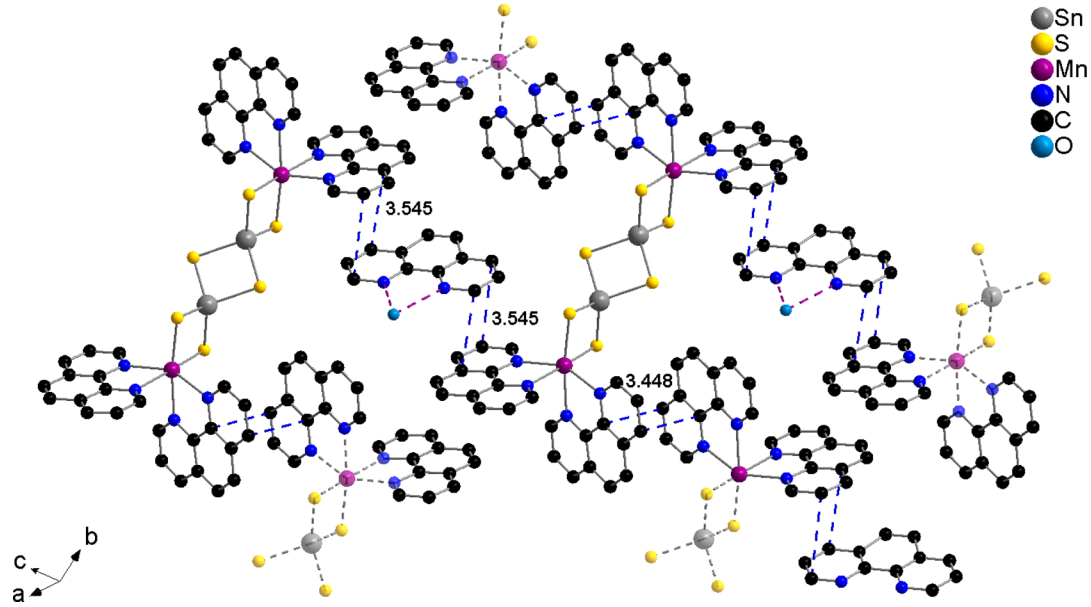

Figure 7. 3D arrangement of the molecules in **4** showing the off-center parallel stacking (blue dashed lines). Hydrogen atoms are omitted for clarity. The dashed lines between O and N atoms indicate hydrogen-bonding interactions.

Compounds **2** and **4** (triclinic, space group $P\bar{1}$, $Z = 1$, Table 1) contain an additional phen molecule (**2**) or a phen molecule and a lattice water molecule (**4**). In the structure of **2**, the $\{[Mn(phen)_2]_2(\mu_2\text{-}Sn_2S_6)\}$ units are joined via off-center parallel stacking interactions along the two different directions [010] (3.599 and 3.572 Å) and [001] (3.479 Å) (Figure 5). The interaction along [001] occurs between slightly staggered molecules (Figure S6, Supporting Information), generating a 3D arrangement with tunnels running along [100]. The tunnels are occupied by phen molecules (Figure S7, Supporting Information) that are disordered over two positions.

A chainlike arrangement of the $\{[Mn(phen)_2]_2(\mu_2\text{-}Sn_2S_6)\}$ moieties along [010] is observed in the structure of compound **4** initiated by off-center parallel stacking arrangement (3.683 Å) along [100] (Figure 6). The not coordinated phen molecule is involved in off-center parallel stacking (3.545 Å) bridging two $\{[Mn(phen)_2]_2(\mu_2\text{-}Sn_2S_6)\}$ moieties in a parallel displaced way developing a 3D arrangement of the constituents (Figure 7). The H_2O molecule seems to interact with the phen molecule via hydrogen bonds, but because the position of the H atoms could not be determined, no further details can be reported.

Compound **5**, $\{[Mn(phen)_2]_2(\mu\text{-}\eta^2\text{-}\eta^2\text{-}SnS_4)_2[Mn(phen)]_2\}\cdot H_2O$, crystallizes in the triclinic space group $P\bar{1}$ with one formula unit in the unit cell. The two crystallographically independent Mn^{2+} ions are in different environments. The Mn1 atom is chelated by two phen molecules and is further coordinated by two S atoms from the $[SnS_4]^{4-}$ anion forming a distorted octahedron. However, the Mn2 atom is coordinated by two N atoms of one phen and three S atoms of two $[SnS_4]^{4-}$ anions in a distorted $[MnN_2S_3]$ trigonal bipyramidal coordination geometry (Figure 8). Two symmetry related trigonal bipyramids share a common edge forming a $[Mn_2S_4N_4]$ dimer with a Mn···Mn separation of 3.262 Å that is shorter than in comparable dimers with Mn···Mn distances between 3.3655 and 3.5984 Å.[45−48] Two $[SnS_4]^{4-}$ anions bridge this dimer with two $[Mn1(phen)_2]^{2+}$ cations via three μ_2-S atoms and one μ_3-S atom forming the neutral molecule (Figure 8). To the best of our knowledge, this is the first example for a $[SnQ_4]^{4-}$ anion (Q = S, Se) connecting two different types of TM^{n+} complex cations in the modes observed here.

The different binding modes of the S atoms influence both the Sn−S bond lengths and S−Sn−S bond angles: The Sn1−S1

dx.doi.org/10.1021/ic500369m | *Inorg. Chem.* 2014, 53, 5619−5630

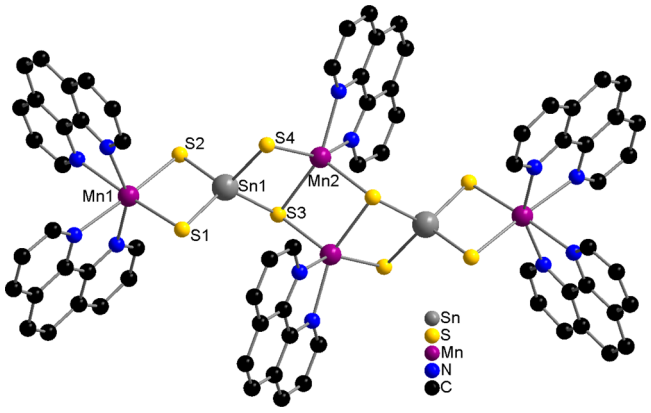

Figure 8. Molecular structure of compound **5**. The hydrogen atoms are omitted for clarity. Only selected atoms are labeled.

and Sn1−S2 bonds are slightly shorter, the Sn−S4 bond is similar, and the Sn1-μ_3-S3 distance is distinctly longer compared to the discrete $[SnS_4]^{4-}$ anion (see Table S8, Supporting Information). The S−Sn−S angles range from 102.17(4)° to 116.12(4)° indicating a severe deviation from the ideal geometry, while discrete $[SnS_4]^{4-}$ thiostannate anions exhibit only small distortions of tetrahedral geometry.[49] Comparable distorted $[SnS_4]^{4-}$ anions were also observed in some thiostannates.[19,24]

In **5**, the units are arranged in chains along the *a* axis and interact via off-center parallel stacking interactions between the central $Mn_2S_4N_4$ moieties (Figure 9). These chains are further connected within the *ac* plane by off-center parallel stacking of the phen molecules of the octahedra $Mn1S_2N_4$ at the periphery of the molecules (Figure 9). The structure analysis gave no hints for a significant interaction between the lattice water molecules and the 2D supramolecular layers.

In comparison to the $[Sn_2S_6]^{4-}$ bitetrahedron, the examples of thiostannates containing the $[SnS_4]^{4-}$ tetrahedron are limited.[19,24,50−52] In addition, the only compound exhibiting a similar bridging function has been observed in the $_\infty^1[MnSnS_4]$ chains of $(1,4\text{-dabH})_2MnSnS_4$, but the ammonium molecules act only as charge balancing ions.[51] Examples for a $[SnQ_4]^{4-}$ anion (Q = S, Se) acting as a tetradentate μ_2-η^2-η^2-ligand bridging two TM^{n+} amine complex cations has been observed in the related class of chalkogenidoarsenates.[53,54]

Variation of the Synthesis Parameters. The successful isolation and characterization of the title compounds as well as the observation that several compounds are transformed with increasing reaction time encouraged us to investigate the compound formation in more detail. Therefore, after isolation of the first compound $\{[Mn(phen)_2]_2(\mu_2\text{-}Sn_2S_6)\}$ (**1**), the reaction time was gradually increased up to finally 8 weeks. In this time window, compound **1** converts within about 3 weeks into $\{[Mn(phen)_2]_2(\mu_2\text{-}Sn_2S_6)\}$ (**3**) that is further converted into $\{[Mn(phen)_2]_2(\mu_2\text{-}Sn_2S_6)\}\cdot phen\cdot H_2O$ (**4**) within 40 days. Obviously, the long reaction times needed to obtain compounds **3** and **4** precluded experiments under static conditions. Hence, we first investigated whether compounds **1**−**4** can be obtained under stirring conditions applying the molar ratio of 1:1:3:2 for the starting materials (compare Table S1, Supporting Information). The advantage of this synthesis route is that the reaction times can be significantly reduced and often the desired products are already obtained after a few hours. In addition, the method is particularly suited to study the influence of various reaction parameters onto product formation within a reasonable time period. But, one should note that sometimes not all compounds nucleate and crystallize under stirring conditions and single crystals cannot be obtained. In the present study, selected reaction parameters such as temperature, pH value, solvent volume, amine concentration,

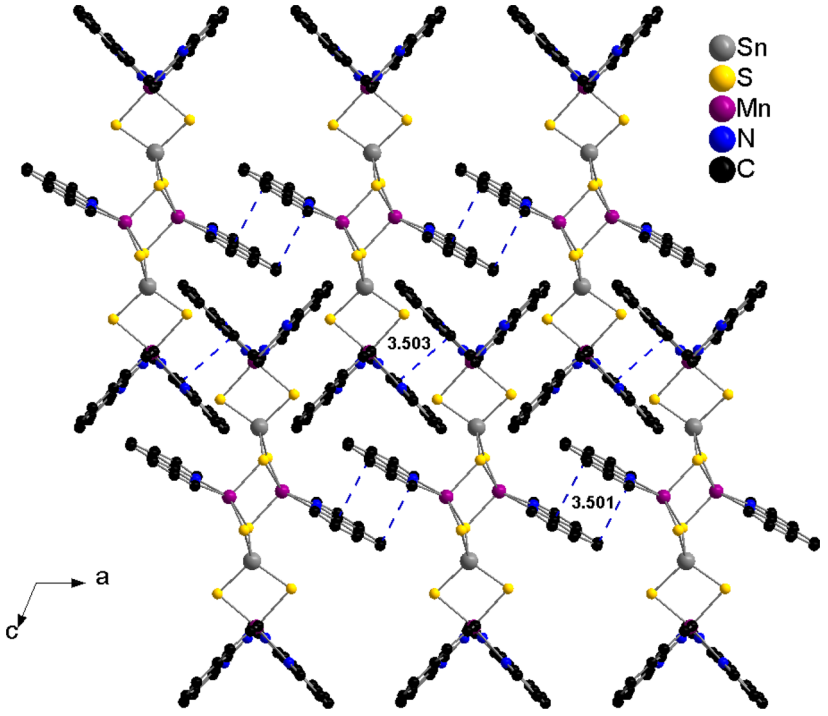

Figure 9. Off-center parallel stacking (blue dashed lines, numbers are the distances between adjacent phen molecules) of the $\{[Mn(phen)_2]_2[\mu_2\text{-}\eta^2\text{-}\eta^2\text{-}SnS_4]_2[Mn(phen)]_2\}\cdot H_2O$ units within the *ac* plane. Hydrogen atoms are omitted for clarity.

dx.doi.org/10.1021/ic500369m | Inorg. Chem. 2014, 53, 5619−5630

Table 2. Compounds that are Obtained if $MnCl_2 \cdot 4H_2O$, Sn, and S are Reacted with Phen at Different Temperatures Using Varying Amine Concentrations[a]

temp	40%	30%	20%	10%
150 °C	1	1	1 + 2 → 3 + 4 → 4	1 → 2 → 4
140 °C	1	1	1 + 2 → 2 → 2 + 3 + 4 → 4	2 → 4
120 °C	1	1	2	2

[a]Note that the pH value for these concentrations is ∼14.

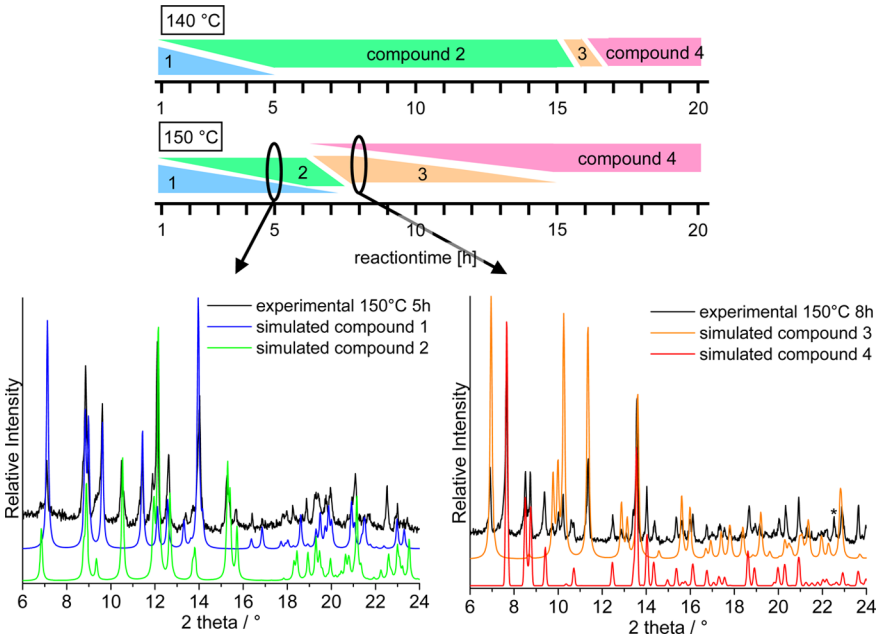

Figure 10. Top: Summary of the formation of the distinct products at an amine concentration of 20% as a function of time at 140 °C (top) and 150 °C (bottom). The pH value was ∼14. Bottom: Selected XRPD pattern of the reaction products after a reaction time of 5 h (left) and 8 h (right) at 150 °C. For further XRPD patterns, see Figures S8 and S9 (Supporting Information).

and reaction time were systematically varied. In the following, the results obtained varying these parameters are discussed.

Influence of Reaction Temperature and Concentration of the Solvent Amine. An increase of the reaction temperature increases the concentration of dissolved species, which has a direct influence on the reaction rate and crystal growth.[55] The temperature does not only affect the kinetics of the reaction but also results in a change of the autogenous pressure,[56] rate of diffusion,[56] viscosity, and dielectric constant of the solvent.[56,57] The latter will also influence the pH of the solution of strong protic solvents.[56] Applying the elements in the syntheses of thiometalates requires the usage of an amine to generate a strong alkaline medium. Elemental sulfur reacts at high pH values to form, for example, polysulfide species, that dissolve the metallic elements.[58−60] Because phen does not provide the necessary pH value, a liquid amine must be supplied. To prevent complex formation with the generated transition metal ions, a monodentate amine, for example, methylamine, is most suitable. Obviously, the pH value of the solution as well as the pressure in the reaction vessel depends on this amine concentration.

As can be seen from Table 2, only compound **1** could be synthesized with the highest amine concentrations (30−40%) independent from the reaction temperature and reaction time. By reducing the amine concentration, a clear effect of the temperature could be observed. At T = 120 °C and amine concentrations of 10% and 20%, only compound **2** is formed for reaction times of 20 h. By increasing the temperature to 140 °C (amine concentration: 20%), a mixture of compounds **1** and **2** is observed for several hours, and **1** disappears after about 5 h (Figure 10). After 16 h, **2**−**4** coexist for about 0.5 h, compounds **2** and **3** disappear, and only **4** is observed as final product. The situation is different at T = 150 °C, where **1** and **2** are simultaneously present up to about 7 h, and for a very short time period, **1**−**4** coexist followed by disappearance of **1** and **2**. Up to about 15 h reaction time, **3** and **4** could be identified in the reaction product, and for t > 15 h, only **4** was observed. The situation is quite different for 10% amine concentration where only compound **2** was observed at T = 120 °C and a conversion of compound **2** into **4** occurs at T = 140 °C. For the highest temperature of 150 °C, compound **1** is observed first for a short time, and then, **2** and **4** are successively formed with increasing reaction time. At this amine concentration, compound **3** was never observed.

As mentioned above, the concentration of the amine in aqueous solution does not only alter the pH value but the pressure in the reaction vessel. Hence, we studied the effect of the pressure onto product formation by gradually reducing the volume of the 30% methylamine solution at T = 150 °C and reaction times t = 15 and 20 h. As can be seen in Table 2, at this concentration and 2 mL of solvent, only **1** could be obtained in the selected time window. For t = 15 h for 1.6−2.0 mL, only **1** crystallized, and at 1.3−1.5 mL, a mixture of **1** and **3** occurs. Further reduction to 1.0−1.2 mL, yielded only compound **3** as reaction product (Figure 11). By increasing the reaction time to 20 h, a mixture of **1** and **3** was observed for a volume of 1.5−1.8

dx.doi.org/10.1021/ic500369m | Inorg. Chem. 2014, 53, 5619−5630

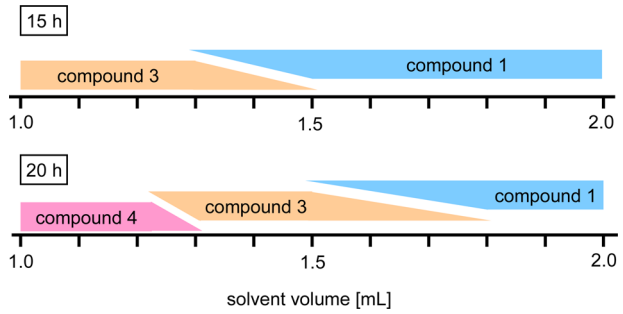

Figure 11. Summary of the formation of the individual products as a function of solvent volume at 15 h (top) and 20 h (bottom). The pH value was ~14. XRPD patterns of the reaction products are displayed in Figures S10 and S11 (Supporting Information).

mL (Figure 10). A further reduction to 1.4 mL achieved only crystallization of **3** while at 1−1.1 mL solution only **4** crystallized. These observations suggest that the conversion of the different compounds is inhibited by higher pressures. Moreover, this series of experiments shows that **2** is only obtained from an amine concentration less than or equal to 20%. But, we cannot exclude that only the pressure is the compound determining factor because a change in concentration of the reactants in solution may also influence the product formation. To verify this, the syntheses were carried out with reduced solvent volume and simultaneously adjusted sample weight. Because these syntheses yield identical results, our hypothesis that the pressure plays the most important role seems to be justified.

It is well documented that $[SnS_4]^{4-}$ tetrahedra are able to condensate to oligomeric anions with the general formula $[Sn_mS_n]^{(2n-4m)-}$,[61a,b] that is, $[Sn_2S_7]^{6-}$, $[Sn_2S_6]^{4-}$, and polymeric $[SnS_3]^{2-}_{\infty}$ species, as well as the adamantane-like $[Sn_4S_{10}]^{4-}$ anion are formed when the pH is reduced.[62] To investigate whether new compounds are formed at lower pH values, further syntheses were carried out keeping the volume of the solvent constant. Interestingly, down to pH = 11, no new compound was formed, but a clear influence on product crystallization of the title compounds was observed (Table 3).

Table 3. Summary of the Observed Compounds in the Variation of the pH Value at Different Temperatures, Constant Volume of 2 mL, and Reaction Times of 5−20 h

temp	pH 14	pH 13	pH 12	pH 11
150 °C	1	1	1 → 3	1 → 3
140 °C	1	1	1	1 → 2
120 °C	1	1	1	2

Regardless of the temperature, only compound **1** was obtained at pH = 13−14. At lower pH values (11−12), however, a significant influence of the temperature is seen. At 150 °C, first compound **1** is formed that then is transformed into **3** after 20 h (pH = 12), while the conversion at a pH = 11 took place about 5 h earlier than at pH = 12. Compound **2** could not be detected for pH = 12−14 at all temperatures. By adjusting the pH value to 11, compound **2** was the only reaction product at T = 120 °C within the selected reaction time range. For the same pH value, a conversion of **1** to **2** occurs at T = 140 °C, and for T = 150 °C, this compound could not be observed but rather the occurrence of **1** followed by conversion into **3**. These observations are in agreement with the results of the concentration studies, in which at low temperatures, also, no conversions were observed and depending on the concentration of the amine compounds **1** and **2** represented the most stable forms. However, compound **4** was not observed under the present reaction conditions.

Investigations on the Thermal Properties and the Transition Behavior. The thermal properties of $\{[Mn(phen)_2]_2(\mu_2\text{-}Sn_2S_6)\}\cdot phen\cdot H_2O$ (**4**) were investigated by simultaneous differential thermoanalysis and thermogravimetry (DTA-TG). In this case, it might be expected that, on heating, water is removed in the first step leading to the formation of $\{[Mn(phen)_2]_2(\mu_2\text{-}Sn_2S_6)\}\cdot phen$ (**2**). On further heating, phen may be emitted, and a transformation into compounds **1** or **3** might be observed. On heating compound **4** with 4 °C/min, three distinct mass steps are observed in the TG curve that are accompanied by three endothermic events in the DTA curve (Figure 12). The experimental mass losses of 1.9% and 12.4%

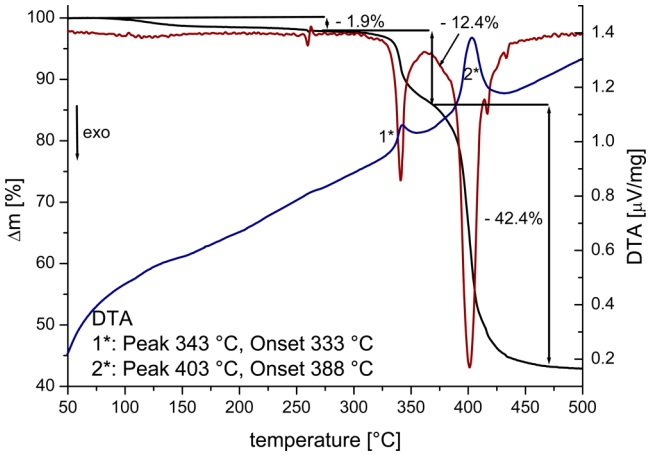

Figure 12. DTA, TG, and DTG curves of compound **4** at 4 °C/min measured in nitrogen atmosphere.

are in reasonable agreement with that calculated for the removal of water in the first and phen in the second TG step ($\Delta m_{calc}(-H_2O$ = 1.2% and $\Delta m_{calc}(-$phen) = 12.4%). In contrast, the mass loss in the third TG step of 42.4% is only in rough agreement with that expected for the removal of the remaining four phen ligands $\Delta m_{calc}(-4$ phen) = 49.3%.

However, from the DTG curve, it is obvious that all mass steps are not well resolved, and therefore, heating rate dependent DTA-TG measurements were performed with 1, 8, and 16 °C/min (see Figure S12, Supporting Information). These investigations clearly demonstrated that the best resolution is obtained with 4 °C/min. In further investigations, additional DTA-TG measurements were performed, and the residues obtained after the first and second TG step at 260 and 360 °C were isolated and investigated by XRPD (Figure 13 and Figure S13, left, Supporting Information). Surprisingly, the X-ray powder pattern of the residue obtained after the first step corresponds to that calculated for **4**. However, the powder pattern of residue isolated after the second TG step at 360 °C corresponds to that calculated for **3** (Figure 13). It is noted that an additional reflection is observed at about 8.9°, which does not correspond to one of the reflections of the second modification **1**, and at the moment, we have no explanation for this observation. However, as mentioned above, the powder pattern of the residue obtained after the first TG step is similar to that of the pristine material **4**. To investigate if compound **2**

dx.doi.org/10.1021/ic500369m | Inorg. Chem. 2014, 53, 5619−5630

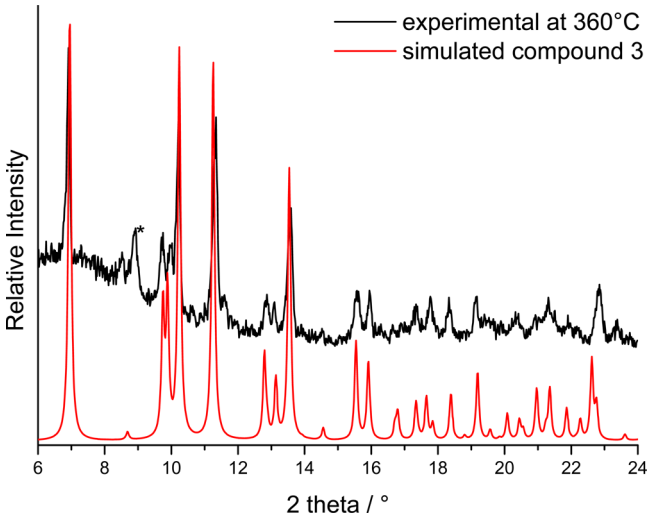

Figure 13. Experimental X-ray powder pattern of the residue obtained after the second TG step at 360 °C and simulated pattern for compound **3** calculated from single-crystal data. The additional reflection that cannot be assigned to one of compounds **1** or **3** is indicated by a star.

can be obtained at higher temperatures, a second TG run was performed and stopped at 340 °C. Comparison of the experimental X-ray powder pattern of this residue with those calculated for all compounds clearly shows that a mixture of compounds **4** and **3** is obtained (Figure S13, right, Supporting Information). Therefore, it can be assumed that the water is removed from **4** without significant structural changes leading to a compound of the same composition as **2**, which in this case represents a further modification.

To gain further knowledge on the thermal behavior of compound **4**, measurements using temperature-dependent XRPD were performed (Figures S14 and S15, Supporting Information). In this case, all reflections of compound **4** disappear at about 315 °C, indicating the formation of an amorphous phase, which does not crystallize on further heating. The discrepancy between the DTA-TG and temperature-dependent XRPD experiments is not surprising because they are performed under different experimental conditions and it is well known that the outcome of a thermal decomposition depends on a number of parameters, for example, the heating rate and the atmosphere used in the measurement.

Investigations on the Stability of Compounds 1 and 3. As mentioned above, thermal decomposition of compound **4** leads to the formation of compound **3** as an intermediate, which exhibits the same composition as compound **1**. Whether they truly represent polymorphic modifications is difficult to decide because the structure of **1** contains small cavities in which no electron density could be located indicating that they are empty (see the Single-Crystal Structure Determination section). In contrast, in **3**, some residual electron density was found in the cavities indicative for the presence of disordered solvent. However, one must keep in mind that **3** can be isolated at 360 °C by thermal decomposition of compound **4**, and hence, it is practically impossible that the cavities are filled with some solvent. Therefore, even if **3** contains some residual solvent, it can be assumed that it can be removed without collapse of the structure, and therefore, it is highly likely that **1** and **3** represent polymorphic modifications. In any case, the question rises which of the two compounds is more stable at room temperature. To answer this question, a solvent-mediated conversion experiment was performed in which a mixture of both forms was stirred in a saturated solution in water with an excess of the solid material. After 2 days, the residue was filtered off and investigated by XRPD measurements, which clearly proves that the mixture is still present (see Figure S16, Supporting Information). This might be traced back to a low solubility of compounds **1** and **3** in water that prevents a transformation into the more stable compound. To determine the solubility of **1** and **3**, a solution of each of the compounds with an excess of solid was stirred for only 1 day in water to exclude any transformation into the more stable compound. Afterward, a distinct volume of the clear solution was

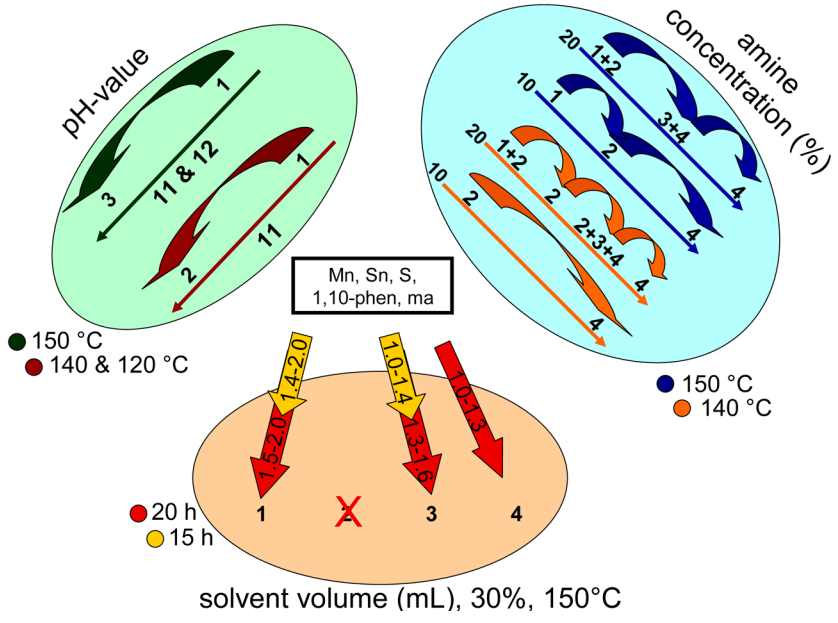

Figure 14. Overview of the results of the investigation of the influence of selected synthesis parameters on the formation of compounds **1**–**4** (see text).

dx.doi.org/10.1021/ic500369m | *Inorg. Chem.* 2014, 53, 5619–5630

investigated by AAS (Table S9, Supporting Information). The result clearly shows that compound **3** is less soluble and therefore should be more stable at room temperature than **1**.

CONCLUSIONS

In the structures of **1**−**4**, a central $[Sn_2S_6]^{4-}$ bitetrahedron bridges two unsaturated $[Mn(phen)_2]^{2+}$ complex cations by the four terminal S atoms to form neutral $\{[Mn(phen)_2]_2(\mu_2\text{-}Sn_2S_6)\}$ moieties, a connection mode never observed for the $[Sn_2S_6]^{4-}$ anion. Compound **5** belongs to the group of less common compounds with a $[SnS_4]^{4-}$ unit acting as a bridging ligand. In addition, in this compound, the $[SnS_4]$ unit exhibits a unique coordination mode.

The results of the systematic study of the influence of synthesis parameters onto product formation are schematically summarized in Figure 14. At high amine concentrations (30−40%) affording high pH values (solvent volume constant of 2 mL), only compound **1** crystallized at T = 120−150 °C. Lowering the concentration to 10−20%, phase pure **2** is obtained at the lowest temperature, while a more complex behavior of occurrence and conversion of the samples are found at higher temperatures and 10−20% amine concentrations. It is remarkable that compound **3** could not be observed under these reaction conditions. The solvent volume also strongly affects nucleation and growth of the individual compounds (t = 20 h). Compound **4** is formed at the lowest volume while **1** is observed at the highest volume. It seems that a high pressure in the reaction vessel suppresses conversion of **1** into the other compounds with time as observed for low amine concentrations and a constant volume of 2 mL. Finally, crystallization of a distinct compound can be controlled by adjusting the pH value. For T = 120 °C and pH = 11, compound **2** crystallized as phase pure material while for T = 140 °C first compound **1** occurs that is then transformed into **2**. The final reaction product at T = 150 °C and pH = 11−12 is compound **3** that appears after **1** disappeared.

The results obtained during the studies are remarkable with respect to several points. Stirring the reaction slurry allows a relatively fast screening of the parameter space of solvothermal syntheses compared to traditional reactions performed for several days. In addition, new compounds can be discovered within reasonable time frames that require long time periods if static conditions are applied. Under stirring conditions, the formation of concentration gradients within the reaction mixtures is avoided yielding phase pure materials if the synthesis parameters are appropriately adjusted. Finally, the results demonstrate the complexity of the solvothermal approach, and only a systematic variation of the synthesis conditions leads to a better understanding of these reactions. The mechanism of the conversion or transformation of the different compounds cannot be deduced from the experiments. Two further interesting results should be shortly highlighted. Compound **5** was only observed in low yield using a Teflon-lined steel autoclave while compound **2** crystallized only in glass tubes. These observations indicate that the surface of the reaction vessel plays an important but yet not understood role for the nucleation of distinct compounds.

The two compounds **1** and **3** are presumably polymorphs and follow the density rule, that is, the density of **3** is larger than that of **1** suggesting that **3** is thermodynamically stable at low temperatures. The compounds **2** and **4** may be viewed as pseudopolymorphs of **1** and **3**.

ASSOCIATED CONTENT

Supporting Information

Experimental and simulated XRPD patterns of **1**−**5** (Figure S1); results of the UV/vis, IR, and Raman measurements of **1**−**5** (Figures S2−S4); illustration of the arrangement of the molecules in the structures **1** and **2** (Figures S5−S7); selected XRPD patterns for the series of time-dependent formation experiments at 140 and 150 °C (Figures S8 and S9, respectively); selected XRPD patterns for the series of solvent volume-dependent formation after 15 and 20 h (Figures S10 and S11, respectively); thermogravimetric curves of compound **4** for different heating rates (Figure S12); powder pattern of the decomposition of **4** at 260 and 340 °C (Figure S13); illustration of an overview of the temperature-dependent XRPD experiments (Figures S14 and S15); powder pattern before and after solvent-mediated conversion experiments of **1** and **3** (Figure S16); an overview of the reaction conditions, an overview of the solvent mixtures, the absorptions of the IR spectra, and data of the signals in the Raman spectra (Tables S1−S4); selected bond length and angles of **1**−**5**, selected bond length and angles of **1** and **3** compared to $Na_4Sn_2S_6{\cdot}14H_2O$, dihedral angles between the phenanthroline moieties for compounds **1**−**5**, and selected bond length and angles of compound **5** compared to $Na_4SnS_4{\cdot}14H_2O$ (Tables S5−S8); results of the solubility measurement of AAS (Table S9) This material is available free of charge via the Internet at http://pubs.acs.org. Structural data have been deposited in the Cambridge Crystallographic Data Centre as publication nos. CCDC 999247 (**1**), CCDC 999248 (**2**), CCDC 999249 (**3**), CCDC 99250 (**4**), and CCDC 999251 (**5**). Copies of the data can be obtained, free of charge, on application to CCDC, 12 Union Road, Cambridge CB2 1 EZ, UK (deposit@ccdc.ca.ac.uk).

AUTHOR INFORMATION

Corresponding Author

*Phone: +49 431 880-2419; fax: +49 431 880-1520; e-mail: wbensch@ac.uni-kiel.de.

Notes

The authors declare no competing financial interest.

ACKNOWLEDGMENTS

Financial support by the State of Schleswig-Holstein is gratefully acknowledged.

REFERENCES

(1) Sheldrick, W. S.; Wachhold, M. *Coord. Chem. Rev.* **1998**, *176*, 211−322.
(2) Sheldrick, W. S. *J. Chem. Soc., Dalton Trans.* **2000**, 3041−3052.
(3) Bu, X. H.; Zheng, N. F.; Feng, P. Y. *Chem.—Eur. J.* **2004**, *10*, 3356−3362.
(4) Feng, P. Y.; Bu, X. H.; Zheng, N. F. *Acc. Chem. Res.* **2005**, *38*, 293−303.
(5) Dehnen, S.; Melullis, M. *Coord. Chem. Rev.* **2007**, *251*, 1259−1280.
(6) Jiang, T.; Lough, A.; Ozin, G. A. *Adv. Mater.* **1998**, *10*, 42−46.
(7) Ahari, H.; Ozin, G. A.; Bedard, R. L.; Petrov, S.; Young, D. *Adv. Mater.* **1995**, *7*, 370−374.
(8) Enzel, P.; Henderson, G. S.; Ozin, G. A.; Bedard, R. L. *Adv. Mater.* **1995**, *7*, 64−68.
(9) Parise, J. B.; Ko, Y. H.; Rijssenbeek, J.; Nellis, D. M.; Tan, K. M.; Koch, S. *J. Chem. Soc., Chem. Commun.* **1994**, 527.
(10) Pienack, N.; Schinkel, D.; Puls, A.; Ordolff, M.-E.; Lühmann, H.; Näther, C.; Bensch, W. *Z. Naturforsch.* **2012**, *67b*, 1098−1106.

(11) Park, Y.; Liao, J. H.; Kim, K. W.; Kanatzidis, M. G. *Inorg. Organomet. Oligomers Polym., Proc. IUPAC Symp. Macromol.* **1991**, *33*, 263−276.
(12) Manos, M. J.; Kanatzidis, M. G. *Inorg. Chem.* **2009**, *48*, 4658−4660.
(13) Sheldrick, W. S. *Z. Anorg. Allg. Chem.* **1988**, *562*, 23−30.
(14) Sheldrick, W. S.; Schaaf, B. *Z. Anorg. Allg. Chem.* **1994**, *620*, 1041−1045.
(15) Schaefer, M.; Kurowski, D.; Pfitzner, A.; Näther, C.; Rejai, Z.; Müller, K.; Ziegler, N.; Bensch, W. *Inorg. Chem.* **2006**, *45*, 3726−3731.
(16) Seidlhofer, B.; Antonova, E.; Wang, J.; Schinkel, D.; Bensch, W. *Z. Anorg. Allg. Chem.* **2012**, *638*, 2555−2564.
(17) (a) Engelke, L.; Schaefer, M.; Schur, M.; Bensch, W. *Chem. Mater.* **2001**, *13*, 1383−1390. (b) Michailovski, A.; Kiebach, R.; Bensch, W.; Grunwaldt, J.-D.; Baiker, A.; Komarneni, S.; Patzke, G. R. *Chem. Mater.* **2007**, *19*, 185−197. (c) Engelke, L.; Schaefer, M.; Porsch, F.; Bensch, W. *Eur. J. Inorg. Chem.* **2003**, 506−513. (d) Antonova, E.; Seidlhofer, B.; Wang, J.; Hinz, M.; Bensch, W. *Chem.—Eur. J.* **2012**, *18*, 15316−15322. (e) Kiebach, R.; Pienack, N.; Ordolff, M.-E.; Studt, F.; Bensch, W. *Chem. Mater.* **2006**, *18*, 1196−1205.
(18) Liu, G.-N.; Guo, G.-C.; Zhang, M.-J.; Guo, J.-S.; Zeng, H. Y.; Huang, J.-S. *Inorg. Chem.* **2011**, *50*, 9660−9669.
(19) Liu, G.-N.; Guo, G.-C.; Chen, F.; Guo, S.-P.; Jiang, X.-M.; Yang, C.; Wang, M. S.; Wu, M. F.; Huang, J. S. *CrystEngComm* **2010**, *12*, 4035−4037.
(20) van Santen, R. A. *J. Phys. Chem.* **1984**, *88*, 5768−5769.
(21) Ostwald, W. *Z. Phys. Chem.* **1897**, *22*, 289.
(22) Sheldrick, G. M. *SHELXS-97, Program for the Solution of Crystal Structures*; University of Göttingen: Göttingen, Germany, 1997.
(23) Sheldrick, G. M. *SHELXL-97, Program for the Refinement of Crystal Structures*; University of Göttingen: Göttingen, Germany, 1997.
(24) Pienack, N.; Näther, C.; Bensch, W. *Eur. J. Inorg. Chem.* **2009**, 1575−1577.
(25) Pienack, N.; Näther, C.; Bensch, W. *Z. Naturforsch.* **2008**, *63b*, 1243−1251.
(26) Zhou, J.; Bian, G.-Q.; Dai, J.; Zhang, Y.; Tang, A.; Q.-Y. Zhu, Q.-Y. *Inorg. Chem.* **2007**, *46*, 1541−1543.
(27) Pienack, N.; Puls, A.; Näther, C.; Bensch, W. *Inorg. Chem.* **2008**, *47*, 9606−9611.
(28) Pienack, N.; Lehmann, S.; Lühmann, H.; El-Madani, M.; Näther, C.; Bensch, W. *Z. Anorg. Allg. Chem.* **2008**, *634*, 2323−2329.
(29) Behrens, M.; Scherb, S.; Näther, C.; Bensch, W. *Z. Anorg. Allg. Chem.* **2003**, *629*, 1367−1373.
(30) Jia, D.-X.; Zhang, Y.; Dai, J.; Zhu, Q.-Y.; Gu, X.-M. *Z. Anorg. Allg. Chem.* **2004**, *630*, 313−318.
(31) Fu, M.-L.; Guo, G.-C.; Liu, B.; Wu, A.-Q.; Huang, J.-S. *Chin. J. Inorg. Chem.* **2005**, *21*, 25−29.
(32) Gu, X.-M.; Dai, J.; Jia, D.-X.; Zhang, Y.; Zhu, Q.-Y. *Cryst. Growth Des.* **2005**, *5*, 1845−1848.
(33) Jia, D.-X.; Dai, J.; Zhu, Q.-Y.; Zhang, Y.; Gu, X. M. *Polyhedron* **2004**, *23*, 937−942.
(34) Zhou, J.; Liu, X.; Chen, G.-Q.; Zhang, F.; Li, L.-R. *Z. Naturforsch.* **2010**, *65b*, 1229−1234.
(35) Wang, Z.; Xu, G.; Bi, Y.; Wang, C. *CrystEng. Comm.* **2010**, *12*, 3703−3707.
(36) Krebs, B.; Pohl, S.; Schiwy, W. *Z. Anorg. Allg. Chem.* **1972**, *393*, 241−252.
(37) Seidlhofer, B.; Pienack, N.; Bensch, W. *Z. Naturforsch.* **2010**, *65b*, 937−975.
(38) Zhou, J.; Liu, X.; Chen, G.-Q.; Zhang, F.; Li, L. R. *Z. Naturforsch.* **2010**, *65b*, 1229−1234.
(39) Kromm, A.; Sheldrick, W. S. *Z. Anorg. Allg. Chem.* **2008**, *634*, 1005−1010.
(40) Martinez, C. R.; Iverson, B. L. *Chem. Sci.* **2012**, *3*, 2191.
(41) Grimme, S. . University of Bonn, Germany. Private communication, TPSS-D3/def2-TZVP method; accuracy of energies calculated with the method is about 5−10%.
(42) (a) Goerigk, L.; Kruse, H.; Grimme, S. *ChemPhysChem* **2011**, *12*, 3421−3433. (b) Grimme, S. *Angew. Chem., Int. Ed.* **2008**, *47*, 3430−3434.
(43) Grimme, S. *WIREs Comput. Mol. Sci.* **2011**, *1*, 211−228.
(44) Grimme, S.; Antony, J.; Ehrlich, S.; Krieg, H. *J. Chem. Phys.* **2010**, *132*, 154104.
(45) Seela, J. L.; Folting, K.; Wang, R.-J.; Huffmann, J. C. G.; Cristou, G. *Inorg. Chem.* **1985**, *24*, 4454−4456.
(46) Seela, J. L.; Knapp, M. J.; Kolack, K. S.; Chang, H.-R.; Huffman, J. C.; Hendrickson, D. N.; G. Christou, G. *Inorg. Chem.* **1998**, *37*, 516−525.
(47) Lin, C.-H.; Chen, C.-G.; Tsai, M.-L.; Lee, G.-H.; Liaw, W.-F. *Inorg. Chem.* **2008**, *47*, 11435−11443.
(48) Tamura, H.; Tanaka, S.; Matsubayashi, G.; Mori, W. *Inorg. Chim. Acta* **1995**, *232*, 51−55.
(49) Schiwy, W.; Pohl, S.; Krebs, B. *Z. Anorg. Allg. Chem.* **1973**, *402*, 77−86.
(50) Pienack, N.; Näther, C.; Bensch, W. *Solid States Sci.* **2007**, *9*, 100−107.
(51) Pienack, N.; Bensch, W. *Z. Anorg. Allg. Chem.* **2006**, *632*, 1733−1736.
(52) Pienack, N.; Möller, K.; Näther, C.; Bensch, W. *Solid States Sci.* **2007**, *9*, 1110−1114.
(53) Liu, G.-N.; Guo, G.-C.; Chen, F.; Wang, S.-H.; Sun, J.; Huang, J.-S. *Inorg. Chem.* **2012**, *51*, 472−482.
(54) Jia, D.; Zhao, J.; Pan, Y.; Tang, W.; Wu, B.; Zhang, Y. *Inorg. Chem.* **2011**, *50*, 7195−7201.
(55) Demazeau, G. *J. Mater. Sci.* **2008**, *43*, 2104−2114.
(56) Rabenau, A. *Angew. Chem.* **1985**, *97*, 1017−1032; *Angew. Chem., Int. Ed. Engl.* **1985**, *24*, 1026−1040.
(57) Schur, M. Dissertation. Johann-Wolfgang-Goethe-Universität, Frankfurt am Main, 1999.
(58) Jiang, T.; Lough, A.; Ozin, G. A.; Bedard, R. L. *J. Mater. Chem.* **1998**, *8*, 733−741.
(59) Schur, M.; Bensch, W. *Z. Kristallogr.* **1997**, *212*, 305−307.
(60) Schur, M.; Bensch, W. *Z. Anorg. Allg. Chem.* **1998**, *624*, 310−314.
(61) (a) Sheldrick, W. S.; Wachhold, M. *Angew. Chem.* **1997**, *109*, 214−234. (b) *Angew. Chem., Int. Ed. Engl.* **1997**, *36*, 206−224.
(62) Krebs, B. *Angew. Chem.* **1983**, *95*, 113−134; *Angew. Chem., Int. Ed. Engl.* **1983**, *22*, 113−134.